Journal of Atmospheric and Solar-Terrestrial Physics 135 (2015) 181–191

Contents lists available at ScienceDirect

Journal of Atmospheric and Solar-Terrestrial Physics

journal homepage: www.elsevier.com/locate/jastp

Research paper

# Impact of the 15 January 2010 annular solar eclipse on the equatorial and low latitude ionosphere over the Indian region

S.K. Panda [a,*], S.S. Gedam [a], G. Rajaram [b,1], S. Sripathi [c], A. Bhaskar [c]

[a] Centre of Studies in Resources Engineering, Indian Institute of Technology Bombay, Mumbai 400076, India
[b] Indian Institute of Geomagnetism, Mumbai 400005, India
[c] Indian Institute of Geomagnetism, Navi Mumbai 410218, India

ARTICLE INFO

*Article history:*
Received 8 March 2014
Received in revised form
4 November 2015
Accepted 5 November 2015
Available online 7 November 2015

*Keywords:*
Solar eclipse
Gravitational tides
Counter electrojet
Total electron content
Equatorial ionization anomaly

ABSTRACT

The annular solar eclipse of 15 January 2010 over southern India was studied with a multi-instrument network consisting of magnetometer, ionosonde and GPS receivers. The presence of a counter electrojet (weakened or westward zonal electric field) during the eclipse and adjacent days suggests the strong gravitational tidal effect associated with the exceptional Sun–Moon–Earth alignment around the eclipse day. With a strong backup of magnetometer recordings on the day of eclipse, its adjacent days and the normal electrojet day, it is argued that the regular eastward electric field for the whole day at the equator was not just weakened, but actually was flipped for several hours by the influence of enhanced lunar tides. The effect of flipping the electric field was clearly seen in the equatorial ionosonde data and through the large array of GPS receivers that produced the total electron content (TEC) data. The main impact of flipping the electric field was poor feeding of equatorial ionization anomaly (EIA) due to the severely weakened fountain effect on the eclipse day, with the regular anomaly crest shifting towards the equator. The equatorial ionosonde profile was also showing an enhanced F2 region peak in spite of a reduced vertical TEC. While the plasma density depletion at the lower F region altitude over the equator was due to the temporary lack of photo-ionization, the reductions in high altitude plasma density beyond the equator were caused by the electrodynamics taking place around the eclipse. The important finding of this analysis is that the electrodynamical consequences on the low latitude ionosphere were mainly due to the combination of eclipse and lunar tides which were far more significant and influenced the EIA density rather than eclipse alone. Based on these findings, it is argued that the prevailing lunar tidal impact also needs to be taken into account while seeking to understand the electrodynamical impact of the solar eclipse on the low latitude ionosphere.



## 1. Introduction

A solar eclipse is of paramount importance for researchers as it provides a unique opportunity to investigate the atmospheric and ionospheric effects caused by the rapidly moving shadow of the Moon over the Earth. The effects associated with solar eclipses can alter the whole electrodynamics of the low latitude ionosphere specially when the eclipse occurs near the dip equator. Nowadays, the availability of simultaneous observations from different ground and space based instruments gives a good opportunity for understanding the changes in the regular electrodynamics during solar eclipse and its consequences at the equatorial and higher latitudes. Although studies have been performed over various parts of the globe to realize the temporal and spatial ionospheric variations with the passage of solar eclipses, their effects over the equatorial and low latitude ionosphere are of unique interest. In view of this, we tried to investigate the response of the equatorial and low latitude ionosphere using multi-instrument network consisting of magnetometer, ionosonde and GPS receivers to the annular solar eclipse of 15 January 2010 as observed over southern India.

The regular electrodynamics of ionosphere near the dip equator is greatly influenced by the enhanced Cowling conductivity. Manifestation of this is seen as an intense current, flowing eastward in the ionospheric E-layer during the daytime, within a narrow belt of $\pm 3°$ latitude over the magnetic dip equator, this current is referred to as the equatorial electrojet (EEJ) (Chapman, 1951). In the vicinity of the dip equator, the EEJ is seen as a daytime enhancement in the horizontal component ($H$) of the

* Corresponding author. Fax: +91 022 25783190.
*E-mail addresses:* sampadpanda@gmail.com (S.K. Panda), shirish@iitb.ac.in (S.S. Gedam), girijarajaram@gmail.com (G. Rajaram), sripathi@iigs.iigm.res.in (S. Sripathi), ankushbhaskar@gmail.com (A. Bhaskar).
[1] Presently associated with Centre of Studies in Resources Engineering, Indian Institute of Technology Bombay, Mumbai 400076, India.

http://dx.doi.org/10.1016/j.jastp.2015.11.004
1364-6826/

geomagnetic field. However, it is also observed that on certain geomagnetic quiet days the EEJ current direction reverses to westward generally during the morning and evening hours, giving rise to a negative depression in magnetometer *H* data. The resulting current is termed as counter electrojet (CEJ) (Gouin and Mayaud, 1967). Any equatorial phenomenon causing disturbance in the net zonal electric field eventually affects the E and F-region and hence the distribution of plasma in the low latitude ionosphere. The total electron content (TEC) measured from the GPS observables is a powerful tool to study the static as well as dynamic characteristics of the F-region plasma and its photochemistry, as the main contribution to the TEC comes from the F-region. The vertical drift of the F region plasma gives rise to the equatorial ionization anomaly (EIA) in the low latitudes. The EIA is characterized by a trough in the ionization density at the geomagnetic equator and crests on either side of the equator within $\pm 15°$ magnetic latitudes (Appleton, 1946). The EIA development is affected by various transient processes like geomagnetic storms, prompt penetration electric fields, solar eclipses, etc. The underlying physical processes during the eclipses can be probed by studying the variations in EEJ, TEC, and related ionospheric parameters.

The effects associated with a solar eclipse are always unique, since the solar eclipses may occur at various geographic locations during different phases of the solar activity, geomagnetic conditions, seasons, as well as local times of the day. Moreover, a particular eclipse does not repeat in any recognizable pattern due to the diverse Sun–Moon–Earth alignment geometries and different lunar orbital characteristics (Espenak and Meeus, 2006); hence the study of individual eclipses becomes necessary. Also, induced ionospheric effects have significant impact on satellite-based trans-ionospheric radio-telecommunication and navigation systems (Vyas and Sunda, 2012). The obscuration of solar radiation during partial, annular or total solar eclipse, leads to spatial and temporal ionospheric and thermospheric variations through the reduced production of electrons and accelerated recombinations (Rishbeth and Garriott, 1969). Ionospheric responses to the earlier solar eclipses have been broadly studied by many researchers across the globe with different techniques, such as incoherent scatter radar (Evans, 1965; Salah et al., 1986), Faraday rotation measurement (Klobuchar and Whitney, 1965), ionosonde (Adeniyi et al., 2007), ground and space based GPS observations (Tsai and Liu, 1999; Tomás et al., 2008), satellite (Cohen, 1984), rocket-borne measurements (Manju et al., 2012, 2014), and magnetometers (Sridharan et al., 2002; Tomás et al., 2008). Model calculations of the eclipse effects have also been carried out by Le et al. (2010) and Lin et al. (2012).

Earlier studies demonstrate the reductions in the ionization during the eclipses, based on the comparison of the solar eclipse day with one or more control days, mainly the previous and succeeding days of the eclipse (Evans, 1965; Adeniyi et al., 2007; Chandra et al., 2007; Manju et al., 2012; Madhav Haridas and Manju, 2012; Kumar et al., 2013). Some studies also have considered mean variations of first five international geomagnetically quietest days (Q-Days) or monthly averages excluding the disturbed days (Sharma et al., 2010; Choudhary et al., 2011; Kumar and Singh, 2012). Sridharan et al. (2002), St.-Maurice et al. (2011), and Choudhary et al. (2011) demonstrated the effects of the eclipse-induced terminators, by using observations and models which are really thought-provoking. Most of the studies ascribe the reduced TEC to the obvious temporary interruptions of the solar radiation due to the obscuration. However, the equatorial dynamics during the eclipse and control days has to be taken into account for a reliable and better physical picture. One has to be careful in selecting control days as studies reveal that the frequency of CEJ occurrence increases during geomagnetically quiet days through changes in the zonal electric field, which are more prevalent during solar minimum solstice months (Mayaud, 1977). This could result in ambiguity when the eclipse observations are compared with the control or quiet days, without verifying the disturbances in the zonal electric field of these days. Note that the disturbances in the zonal electric field are reflected in the magnetometer EEJ data. Therefore, some information of the equatorial ionosphere can be derived based on the EEJ strength. Hence, the present study is based on due consideration of the EEJ strengths during the eclipse as well as during the control days.

The eclipse of 15 January 2010 gave a unique opportunity to understand the changes in the electrodynamics of the ionosphere during the passage of the Moon's shadow across the Indian region. The eclipse took place during the solar minimum, in the ascending phase of the 24th solar cycle. The geomagnetic condition was very quiet. It happened to be the longest annular eclipse of the 3rd Millennium with the maximum duration of annularity 11 min 08 s (its duration will not be exceeded until the year 3043). It was visible over a 333 km wide track covering almost half of the Earth (Espenak and Meeus, 2006). The annularity was clearly visible from South Kerala and South Tamil Nadu in India, while other parts of the Indian region witnessed only a partial eclipse. The major attraction of the present solar eclipse is that it occurred during the early afternoon hours, i.e., peak ionization time over the Indian EIA region. Also, the path of the annularity crossed the dip equator over the peninsular part of India.

Though there are numerous studies on the occurrence of CEJ during quiet days, very few investigations have tried to understand the physical mechanism of CEJs occurring during solar eclipses (Tomás et al., 2008; Bhaskar et al., 2011). Therefore, it is still a controversial issue, whether the CEJ is induced/modulated by the effects associated with reduced radiation during the eclipse or it is due to the enhanced lunar tidal forces. Also, it could be a superposition of both effects. We believe that adopting different criteria for the selection of control days gives rise to variations in the inferences drawn from the studies. What was unique about this particular solar eclipse is that it crossed the dip equator during the peak hours of the day, when the EIA development was supposed to be in its progressive state. Therefore, in the present work, we set our main objectives of the eclipse study, as (1) to probe the underlying mechanism of the CEJ that occurred during the eclipse, (2) investigate the influence of prevailing electrodynamics on the behavior of ionospheric electron densities, and (3) examine latitudinal variations of TEC to assess the possible impact of anomalous electrodynamics on the fountain effect and hence the EIA. The availability of global geomagnetic and interplanetary parameters, local magnetometer, ionosonde, and the large array of GPS receivers gave us an opportunity to investigate these objectives with a modern multi-instrument study. The comprehensive presentations of Rastogi (1989), Choudhary et al. (2011), St.-Maurice et al. (2011), Madhav Haridas and Manju (2012), and Manju et al. (2012, 2014) motivated to investigate the peculiar ionospheric aspects of the exceptional eclipse configuration during the period.

## 2. Data used and methods of treatment

The locations of magnetometer (blue square), ionosonde (black square), and GPS (red dot) observation stations used in this study are marked on a map showing the path of the solar eclipse in Fig. 1 (modified from Espenak and Anderson, 2008). The corresponding geographic and geomagnetic coordinates, as well as the dip angle of the locations, are listed in Table 1. The onset time of the eclipse, time of centrality, and the end time of the eclipse, along with the obscuration magnitudes at the observation stations are shown in Table 2. Note that annularity was observed at Trivandrum and

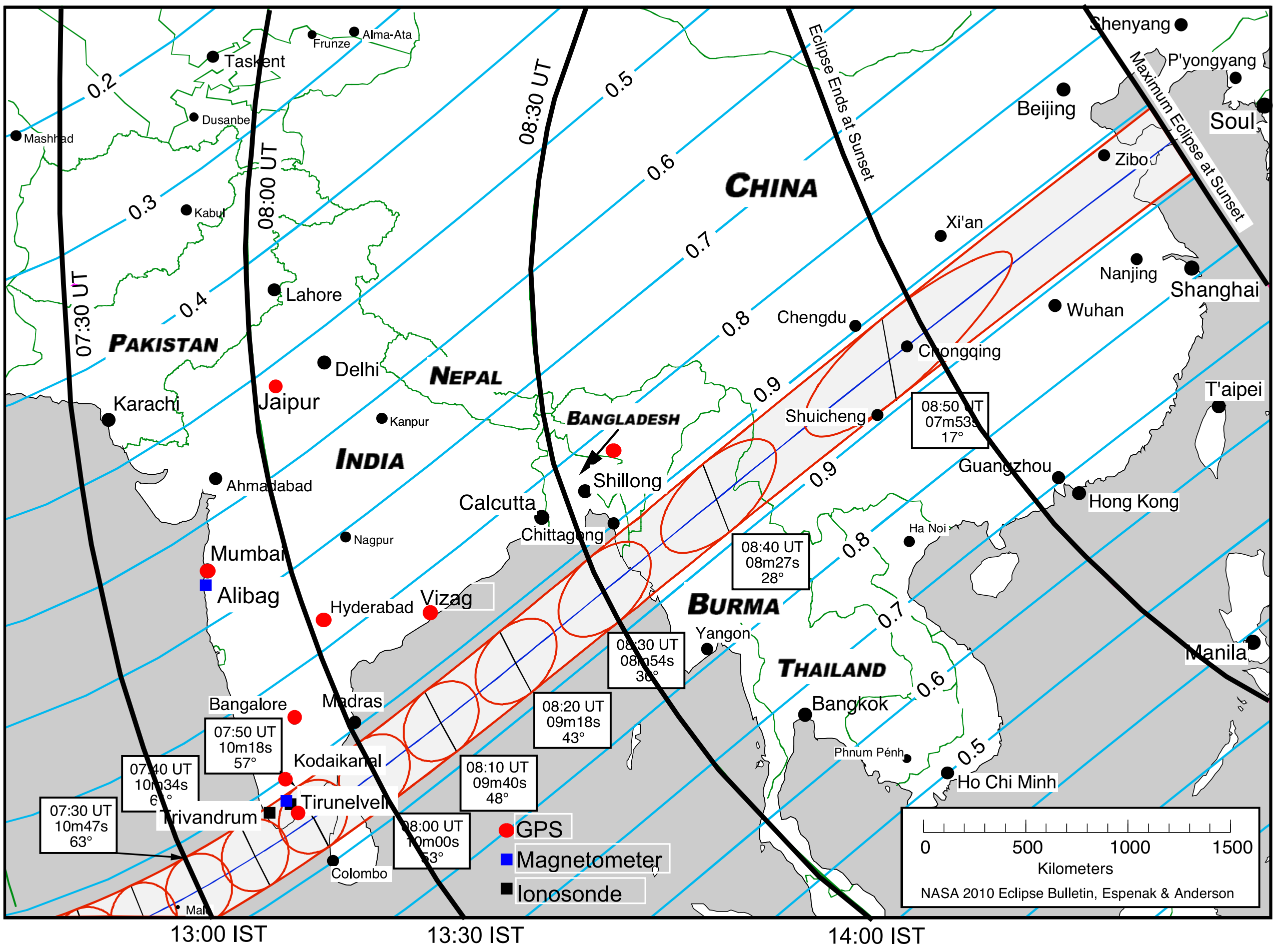


**Fig. 1.** Locations of magnetometer (blue square), ionosonde (red square), and GPS receiver (red dot) stations and path of the annular solar eclipse of 15 January 2010, modified from Espenak and Anderson (2008). (For interpretation of the references to color in this figure caption, the reader is referred to the web version of this paper.)

**Table 1**
Geographic and geomagnetic co-ordinates and dip angle at observation stations and respective instruments.

| Station name | Geographic | | Geomagnetic | | Dip angle | Observations used |
|---|---|---|---|---|---|---|
| | Lat. | Long. | Lat. | Long. | | |
| Trivandrum (TM308) | 08.54 | 76.87 | 0.11S | 149.46 | 2.36 | ION |
| Tirunelveli (TIR) | 08.70 | 77.80 | 0.03S | 150.39 | 2.67 | MAG, ION, GPS |
| Kodaikanal (KODI) | 10.23 | 77.46 | 01.52N | 150.20 | 6.44 | GPS |
| Bangalore (BAN2) | 13.03 | 77.51 | 04.29N | 150.49 | 13.14 | GPS |
| Hyderabad (HYDE) | 17.42 | 78.55 | 08.55N | 151.87 | 23.03 | GPS |
| Vizag (VSKP) | 17.74 | 83.33 | 08.50N | 156.49 | 23.43 | GPS |
| Alibag (ABG) | 18.62 | 72.87 | 10.24N | 146.53 | 25.94 | MAG |
| Mumbai (PANV) | 19.01 | 73.10 | 10.60N | 146.80 | 26.74 | GPS |
| Shillong (SHIL) | 21.56 | 91.86 | 15.79N | 165.07 | 31.1 | GPS |
| Jaipur (JAIP) | 26.87 | 75.82 | 18.14N | 150.16 | 41.39 | GPS |

ION, ionosonde; MAG, magnetometer; and GPS, Global Positioning System.

Tirunelveli, whereas at Jaipur the obscuration magnitude was below 50%, the lowest among all stations used in this study. A brief outline of the data and methodology used in our study is set out below. The time used throughout the study is in Indian Standard Time (IST=UT+5:30), as indicated in the figures/tables.

### *2.1. Interplanetary and geomagnetic parameters*

To assess the interplanetary and geomagnetic conditions during the eclipse, we examined the 1-min SYM-H (equivalent to hourly disturbance storm time (Dst) index), the vertical component of the interplanetary magnetic field (IMF-Bz), interplanetary electric field (IEF), and the 3-hourly Kp index. Note that SYM-H represents the ring current strength and therefore acts as a proxy for the strength of magnetospheric disturbances.

As described in the Introduction, the magnetometer *H* variation over the equator is related to the *East* ⇌ *West* ionospheric electric current, and hence is a proxy for the strength of EEJ at the equator. The Tirunelveli (TIR) magnetic observatory is in the vicinity of the EEJ, being located close to the dip equator with EEJ effects superimposed on the worldwide solar quiet (Sq) field, whereas the

**Table 2**
Local circumstances and percentage deviation of TEC during annular solar eclipse of 15 January 2010 from the normal EEJ control day (CD1; 2 January 2010) and preceding control day (CD2; 14 January 2010) at different locations and their comparisons with the earlier reports.

| Station | Start | Maximum | End | Obscuration | Δ% TEC(↓)(Our Observations) | | Δ% TEC(↓)(Others) |
|---|---|---|---|---|---|---|---|
| | | | | | 2 January 2010(CD1) | 14 January 2010(CD2) | |
| Trivandrum | 11:04 | 13:14 | 15:05 | 0.844 | NA | NA | 10–15[a] |
| Tirunelveli | 11:08 | 13:17 | 15:06 | 0.844 | 25 | 31 | NA |
| Kodaikanal | 11:10 | 13:18 | 15:08 | 0.833 | 30 | 32 | NA |
| Bangalore | 11:16 | 13:23 | 15:11 | 0.772 | 39 | 35 | 20[b], 15–30[a] , 40[c], 30[d] |
| Vizag | 11:44 | 13:43 | 15:22 | 0.778 | 56 | 42 | 20-35[a] |
| Hyderabad | 11:29 | 13:32 | 15:15 | 0.688 | 48 | 18 | 25–35[a] , 32–36[c] |
| Mumbai | 11:17 | 13:19 | 15:05 | 0.545 | 46 | 23 | 36–63.8[e] |
| Shillong | 12:19 | 14:04 | 15:32 | 0.752 | 45 | 47 | 10–20[a], 12.9–63.6[e], 56–62[c] |
| Jaipur | 11:45 | 13:34 | 15:09 | 0.426 | 52 | 45 | 10[a], 12.8–60.1[e] |

Time is in IST(UT+5:30).
CD1: Normal EEJ Control Day and CD2: Preceding Control Day.
[a] Vyas and Sunda (2012).
[b] Galav et al. (2010).
[c] Kumar and Singh (2012).
[d] Madhav Haridas and Manju (2012).
[e] Momani et al. (2010).

Alibag (ABG) magnetic observatory is in an off-equatorial low latitude station, mainly influenced by the global Sq current system. In the present study, the EEJ is calculated by subtracting nighttime baseline $H$ from the daytime value and then finding the difference between the two stations, to ensure the removal of magnetospheric and Sq contributions. Therefore, the EEJ strength is defined as:

$$EEJstrength = \Delta H_{TIR} - \Delta H_{ABG} \quad (1)$$

where $\Delta H_{TIR}$ and $\Delta H_{ABG}$ are magnetic field variations at TIR and ABG respectively. This method was earlier suggested by Chandra et al. (1971) and later used by several workers (Rastogi and Klobuchar, 1990; Manoj et al., 2006; Sripathi and Bhattacharyya, May 2012; Bhaskar and Vichare, 2013). The present study uses this EEJ strength to investigate the electrodynamics of the equatorial ionosphere during the eclipse and the control days.

### 2.2. Ionosonde data

The F region parameters (10 min resolution) were measured by two different equatorial ionosonde stations, Trivandrum (Digisonde Portable Sounder 4D; 0.5–30 MHz) and Tirunelveli (Canadian Advanced Digital Ionosonde; 2–20 MHz). The importance of simultaneous consideration of these two stations is that they are situated (1) on the equatorial belt and (2) in the umbral shadow zone of the annular solar eclipse. Having the combined data helps avoiding any troubles related to malfunctions in the instruments and provides an unambiguous understanding of the eclipse-induced changes in (a) equatorial electrodynamics governed by $[E \times B]$ drift and diffusion and (b) ionospheric processes (such as recombination loss, reduced production, etc). The F-region electron density is the major contributor to the ionospheric TEC derived from the GPS observables and other techniques. Hence, a detailed inspection of the F region parameters (foF1, foF2, and hmF2) is carried out in the present study.

### 2.3. GPS-derived TEC

Continuous operation of a network of GPS receivers offers an excellent opportunity for exploring spatial and temporal variations of TEC over the globe. The TEC is quantified by counting the number of electrons in a vertical column with a cross sectional area of $1\,m^2$ and is measured in a unit called TECU, where $1\ TECU = 1_* 10^{16}\ electrons/m^2$ (Klobuchar, 1991). In this study, we examine the behavior of ionospheric TEC derived from dual frequency GPS data in the Indian region at Tirunelveli, Kodaikanal, Bangalore, Hyderabad, Vizag, Mumbai, Shillong, and Jaipur during the eclipse and control days (geophysical parameters are listed in Table 1). The GPS stations at Bangalore and Hyderabad are under the International GNSS Service (IGS) network. Recorded data at the Tirunelveli, Vizag, Mumbai, Shillong, and Jaipur GPS stations are obtained from the Indian Institute of Geomagnetism, Navi Mumbai, India. The GPS station at Kodaikanal is operated by the Indian Institute of Astrophysics, India. Observation data from all these stations are processed using the GPS-TEC analysis application software, developed by Seemala and Valladares (2011). The software algorithm calculates a line-of-site TEC, i.e., the slant TEC (STEC) along the ray path, using the differential phase advance and group delay measurements of GPS L1 (1575.42 MHz) and L2 (1227.60 MHz) frequencies. The TEC corresponding to a particular group delay can be written as:

$$TEC_{group} = \frac{1}{40.3}\left(\frac{f_1^2 f_2^2}{f_1^2 - f_2^2}\right)(P2 - P1) \quad (2)$$

here $P1$ and $P2$ are the pseudoranges (groups) corresponding to GPS frequencies $f_1$ and $f_2$. Similarly, the relative phase TEC can be estimated from the phase measurements on the two frequencies as:

$$TEC_{phase} = \frac{1}{40.3}\left(\frac{f_1^2 f_2^2}{f_1^2 - f_2^2}\right)(\Phi 1 - \Phi 2) \quad (3)$$

where $\Phi 1$ and $\Phi 2$ are phases of carrier frequencies $f_1$ and $f_2$ respectively.

The TEC as derived from differential group delays have large uncertainties due to high noise. Hence, they are smoothed by carrier phase leveling. However, the estimated TEC from the above method is actually the STEC which is then converted into its vertical equivalent (VTEC), using a single layer model mapping function (Schaer, 1999). To minimize the changes in satellite geometry, and the effect of multipath and other lower atmospheric attenuations, an elevation threshold of 30° is fixed at an altitude of 350 km for getting the VTEC from the STEC at the ionospheric pierce points (IPPs).

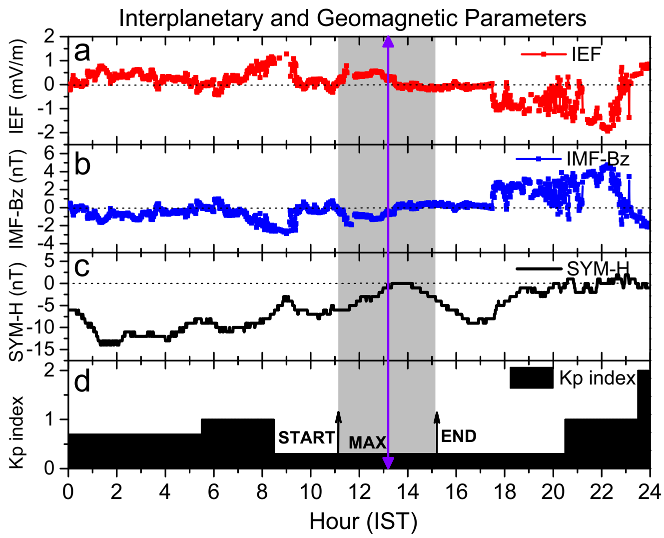


**Fig. 2.** Interplanetary and geomagnetic parameters during 15 January 2010 annular solar eclipse. Panels (a), (b), (c), and (d) depict interplanetary electric field (IEF), interplanetary magnetic field (IMF-Bz), SYM-H index, and Kp index respectively. The shaded region outlines the eclipse duration, with arrows indicating start, maximum, and end of the eclipse.

## 3. Results and discussion

### 3.1. Interplanetary and geomagnetic parameters

Fig. 2 depicts the interplanetary (IEF and IMF-Bz) and geomagnetic field (Kp and SYM-H) parameters on the eclipse day. It is clear from the figure that the maximum Kp index did not exceed 2 and the $\Sigma$Kp index was 8 on the day. The maximum negative excursion of the SYM-H index was around −14 nT. The IMF-Bz had a small magnitude ranging between −5 and 5 nT. Similarly, the variation of the interplanetary electric field is seen to be ranging from −2 to 2 mV/m. From the above observations, it is confirmed that there was nothing unusual with the solar wind and geomagnetic activity. Hence, the day of the eclipse qualifies as a quiet day.

### 3.2. EEJ strength

In Fig. 3(a) we present the hourly EEJ strength for the eclipse and its adjacent days, as well as the top 5 international quietest days (Q-Days) of the month. It can be observed from the figure that the EEJ was considerably weakened or reversed for three consecutive days, with the largest effect being witnessed on the eclipse day in spite of geomagnetically quiet conditions. The other important observation on the eclipse day is that the reversal of the EEJ strength started shortly before the eclipse itself and the strongest CEJ is felt about 1 h after maximum phase of the eclipse. Therefore, the CEJ on the eclipse day is not due to the eclipse itself, rather it must have to do with the alignment of the Sun with the Moon, which suggests that the CEJ around the eclipse day is due to strong gravitational tides. Evidence for the existence of CEJ around the New and Full Moon has been earlier presented by Rastogi (1989) and Tomás et al. (2008). In connection to this, we also verified the EEJ strengths of the Full Moon and New Moon days of two previous and successive months of January 2010 in Fig. 4 and found favorable occurrences of suppressed EEJ strength or CEJ on most of those days. This implies that since a solar eclipse occurs during the New Moon a CEJ formation is favored, particularly with the passage of the lunar shadow over the dip equator.

### 3.3. Control and quiet days

In connection to the present eclipse event, we studied the diurnal EEJ variation for the year 2010 and found a maximum occurrence of suppressed EEJ strength or CEJ during the month of

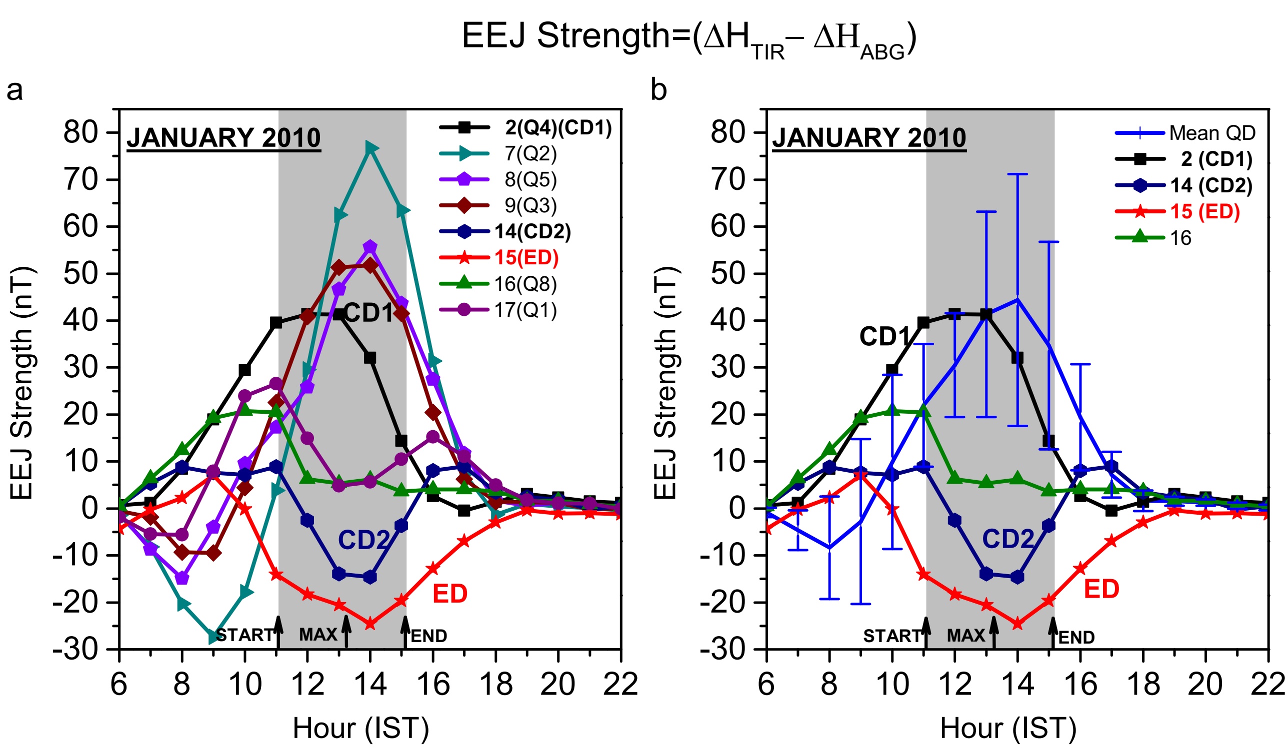


**Fig. 3.** Equatorial electrojet (EEJ) strength over Indian region. (a) On the eclipse day (ED; 15 January 2010), possible control days, and 5 Q-Days of the month. (b) On the eclipse day (ED; 15 January 2010), its succeeding day (16 January 2010), control days (CD1: 2 January 2010 and CD2: 14 January 2010), and average of 5 Q-Days of the month.

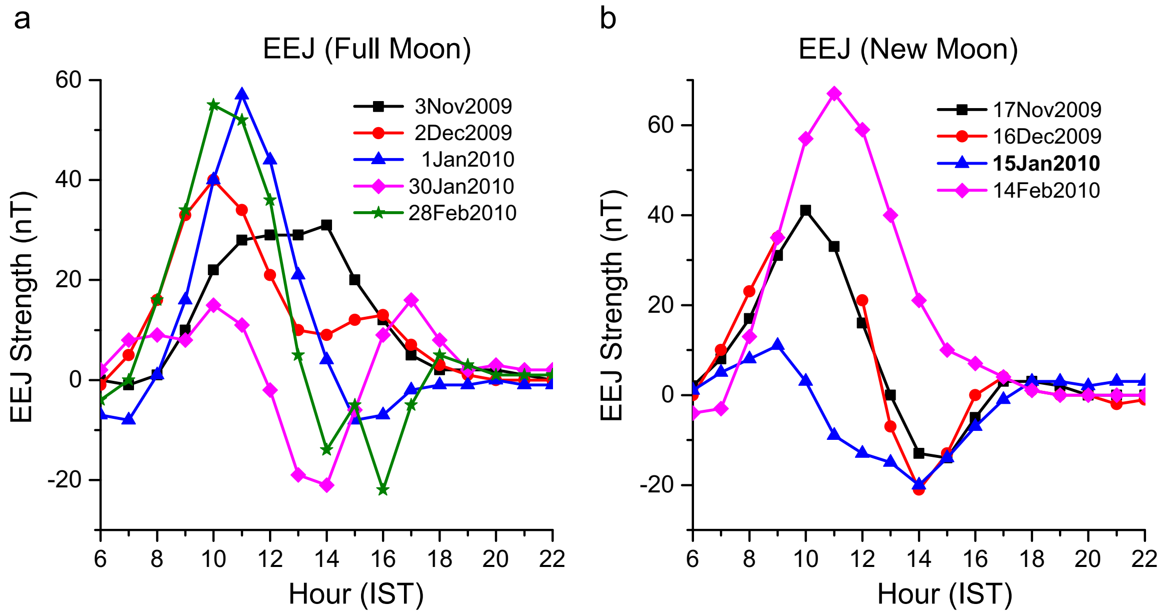


**Fig. 4.** Equatorial electrojet (EEJ) strength over Indian region during the Full Moon and New Moon days in the four adjacent months of January 2010. Observations in March 2010 is left blank as the EEJ strength cannot be calculated due to data outages at the Tirunelveli station.

January. Additionally, the majority of the international Q-Days of the January month also were subject to suppressed EEJ or CEJ effects either in the morning or afternoon hours. The physical reasons behind such equatorial phenomena may have many facets. In Fig. 3(b), we plotted the mean EEJ strength of the top 5 Q-Days of January, which produced a reduced intensity during the morning hours with a shift in the EEJ peak away from the regular noontime.

It is important to note that the international Q-Days are deduced from the Kp indices and may not constitute a quiet behavior at the equatorial and low latitude in terms of electrodynamic prospectives. This is because possible disturbances in the zonal electric field even on a quiet day may alter the equatorial plasma drift and subsequent diffusion at farther latitudes. Therefore, without accounting for these disturbances, one cannot get a complete picture of electrodynamics during the eclipse solely based on the international Q-Days. Perturbations in the zonal electric field can be inferred from the EEJ data, e.g., occurrence of CEJ indicates the reversal/weakening of the eastward zonal electric field. Hence, in the present study we analyzed the EEJ strengths of

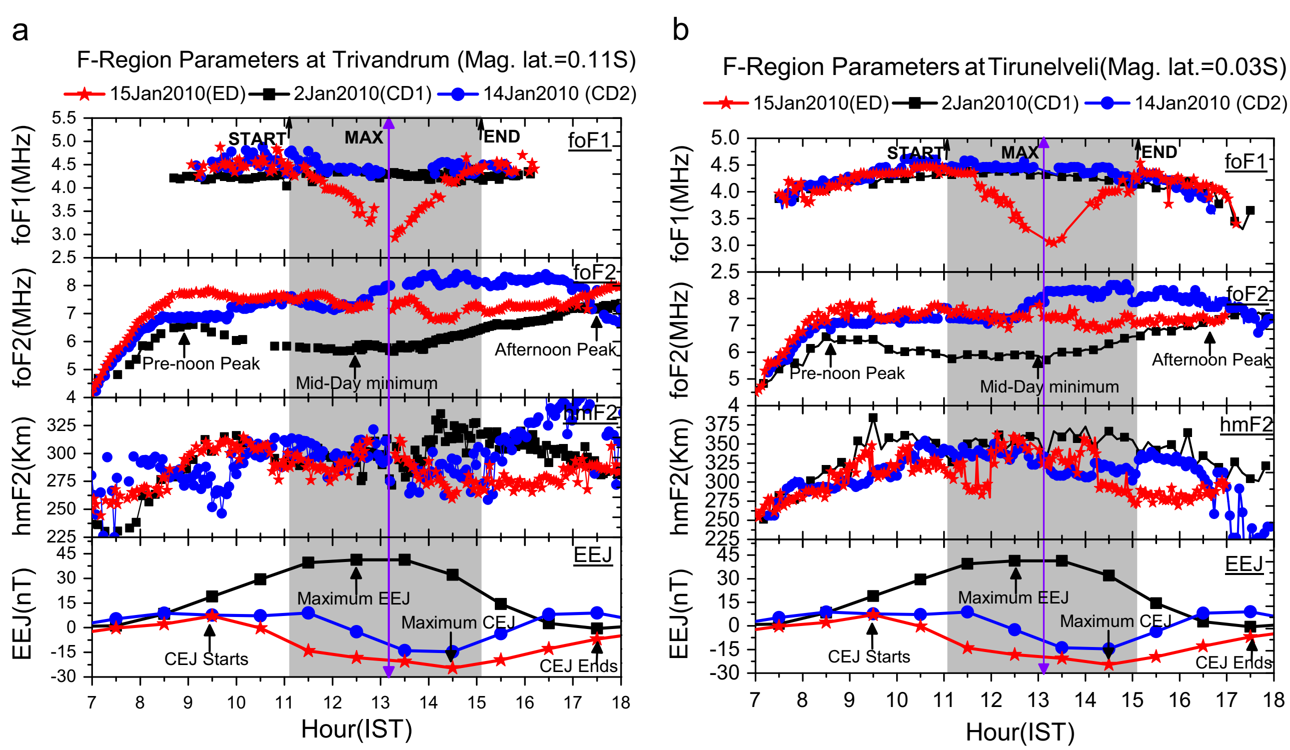


**Fig. 5.** Temporal variations of foF1 (top panel), foF2 (second from top), hmF2 (second from bottom) and their comparison with the control days recorded from the ionosondes at (a) Trivandrum and (b) Tirunelveli. The lower panel in both the columns shows the temporal variations of EEJ strength during the respective days. The shaded region outlines the eclipse duration, with arrows indicating start, maximum, and end of the eclipse.

possible control/Q-Days, amongst which we selected two different control days: (1) the preceding day (14 January 2010) and (2) a very normal electrojet day (2 January 2010). The preceding control day exhibits a similar pattern of CEJ but with a relatively weaker strength as compared to the eclipse day, whereas the normal electrojet day certifies a regular EEJ strength and normalcy in pattern. Quantitatively, a normal EEJ day in the January of year-2010 (low solar activity winter solstice month) can be defined as having a clear positive value of EEJ around 40 nT and peaking near local noon following the apparent movement of the Sun. Considering only the adjacent days of the eclipse day or the mean of international Q-Days of the month might not always be sufficient to probe the electrodynamics during the eclipse. Therefore, the selection of two control days, one with a similar CEJ tendency as that of the eclipse day and the other with a normal EEJ strength qualifying a quiet day, may help in understanding the electrodynamics during the eclipse.

### 3.4. Variations of F-region parameters

Fig. 5 depicts the F-region parameters (top three panels) at Trivandrum and Tirunelveli along with the variation in the EEJ strength (bottom panel) on the eclipse day and on the control days. Both stations show nearly identical foF1 signatures (gradual depletions) clearly related to the eclipse obscuration, as expected from their proximity to one another. This suggests that the equilibrium at the foF1 region is completely disturbed by the lower photo-ionization rate and the continued recombination during the eclipse. The largest differences between the two ionosondes are with hmF2, which is the noisiest information extracted on the eclipse day. The hmF2 decreased abnormally after 09:30 IST for a period of about 2 h and then experienced abrupt upward transitions, centered on the peak obscuration. There is no data available at the central eclipse. However, hmF2 near central eclipse shows an increasing trend. It has been discussed earlier by St.-Maurice et al. (2011) in terms of eclipsed-induced Pre-reversal-enhancement (PRE) generated through a superposition of the low (cooling) and high pressure (solar heating) wind systems during the eclipse. Later, Choudhary et al. (2011) also supported their arguments by retrieving the direction and amplitude of the plasma drift at the equator from a numerical 1-D model.

The most interesting information derivable from the F2-region is that the foF2 is stronger than the normal as well as the preceding day much before the start of the eclipse. The obvious reason is that plasma could not move upward during a counter-electrojet. It spreads out less and the foF2 therefore increases at the equator. After the eclipse has crossed the region, the foF2 is weaker on the day of the eclipse than the preceding day. This may well be due to (a) the absence of plasma production during the eclipse itself and (b) failure in recovering the regular ionization after the end of the eclipse as the Sun had already moved westward. With less plasma having been produced to feed the F region, the F peak would be smaller. Therefore, this difference with the previous day may not be due to the downward push of the plasma, rather it could be due to the reduced photo-ionization during the eclipse and the subsequent hours.

### 3.5. Variations of TEC at equator

To complement the ionosonde observations at equatorial station Tirunelveli, we plotted the GPS-derived TEC data along with the obscuration magnitudes (top) and the EEJ strengths (bottom) in Fig. 6. It is clear from the figure that the TEC on the 14th of January has a noon peak and remains higher than normal. This is consistent with a reduction in the fountain effect related to downward or smaller upward drifts than normal. If the plasma is

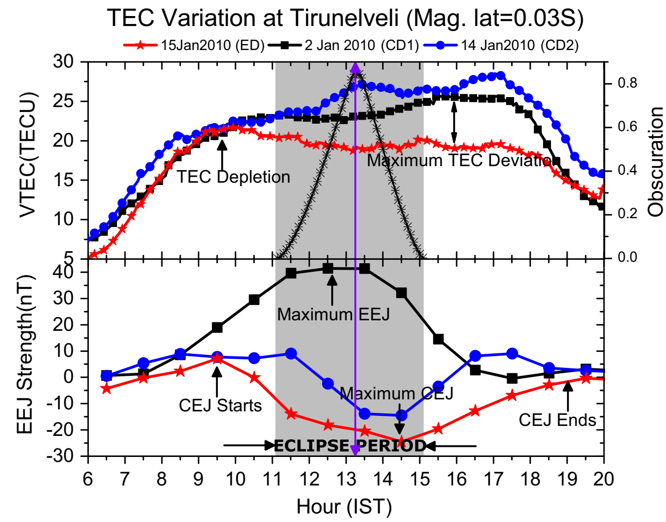


**Fig. 6.** Temporal variations of VTEC and EEJ strength at Tirunelveli during the eclipse day (ED; 15 January 2010) and their comparisons with the normal EEJ control day (CD1; 2 January 2010) and the preceding control day (CD2; 14 January 2010). The black line with stars shows the variations in obscuration magnitude. The shaded region outlines the eclipse duration with a two-headed arrow in the middle which signifies the centrality of the eclipse. The small black arrows indicate maximum amplitudes of EEJ/CEJ.

not feeding the fountain effect, the VTEC at the equator is enhanced. However, the day of the eclipse reveals a smaller VTEC than normal instead of a larger amount on the day before, particularly after 09:30 IST. It is shortly before the eclipse itself. The starting time of VTEC reduction matches well when the CEJ starts on the eclipse day. The smaller VTEC on eclipse day therefore seems to be due to the lack of plasma production during the eclipse and the far stronger CEJ than the day before, which pushes the plasma down hard enough to lead to more plasma recombination from the lower altitudes. A remarkable explanation has been given by Choudhary et al. (2011) in support of extended downward movement of F-region plasma on the eclipse day through running a 1-D model, which includes the associated dynamics and chemistry.

### 3.6. Variations of TEC at higher latitudes

In Fig. 7, we show the temporal variations of VTEC at different latitudes across the Indian region on the eclipse and the control days. The respective obscuration magnitudes, start, maximum, and end time of the eclipse, and the departures of VTEC from the control days are provided in Table 2. It can be observed from Fig. 7 that the VTEC on eclipse day is substantially smaller at all studied stations with respect to the control days. However, the VTEC up to Bangalore (Geomag. latitude: 4.29N) has a behavior similar to the equatorial VTEC on the eclipse day and the day before. This reduced TEC near the equator indicates role of chemistry during the eclipse. At farther latitudes from the equator, the eclipse day deviations from the preceding control day appear to be slightly less than the deviations from the normal EEJ control day. This is predominantly attributed to the weakened fountain effect and poor feeding of the EIA on the preceding day, which become more prominent on the eclipse day forcing a large portion of the lower F-region plasma downward during most of the afternoon hours. The larger deviation of the eclipse day TEC from the normal day TEC around Vizag (Geomag. latitude: 8.50N) confirms that its latitude falls in the vicinity of the regular EIA crest (around 10° for the season). The normal VTEC level at this station could not be

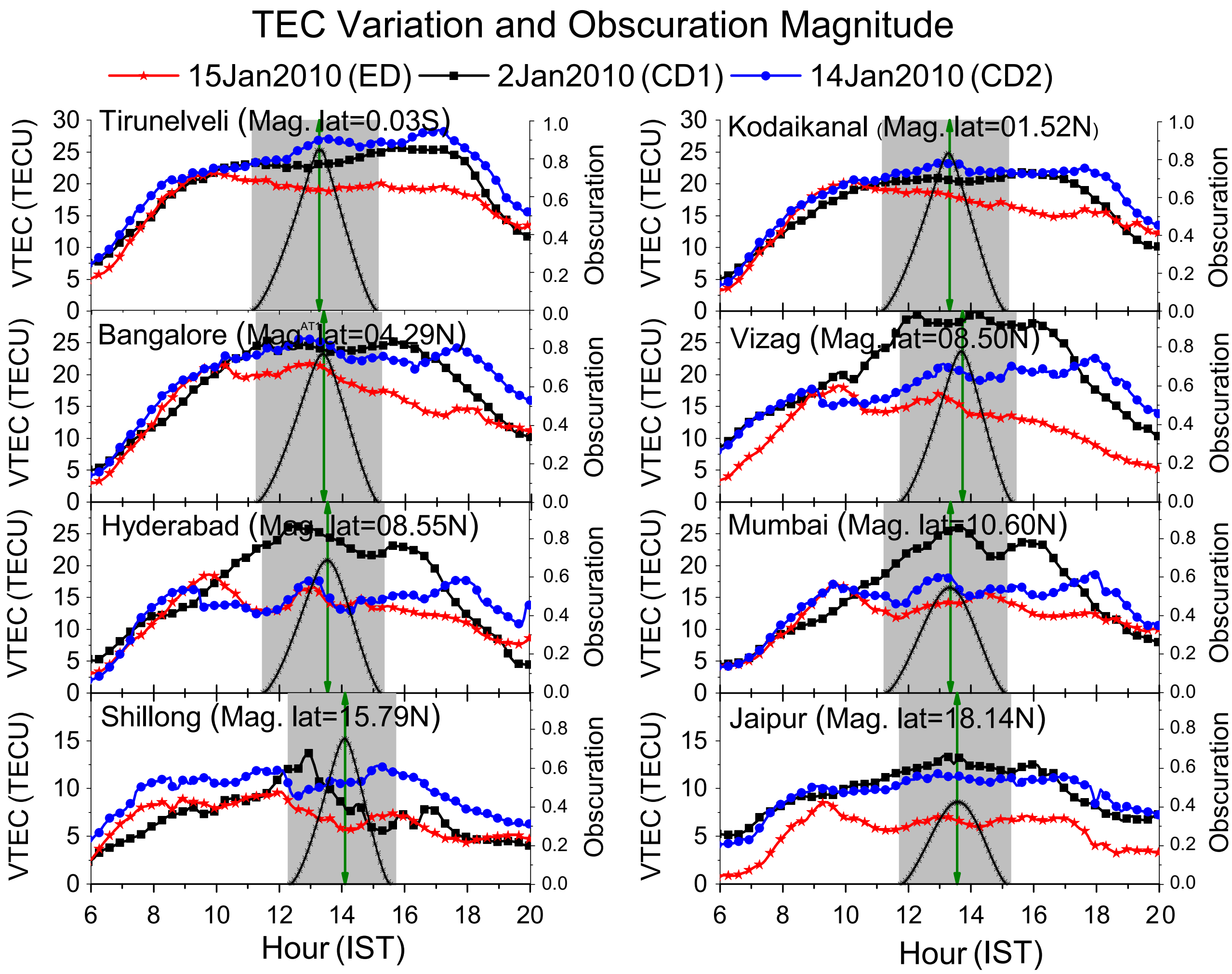


**Fig. 7.** Temporal variations of VTEC and obscuration magnitude at different locations during the eclipse day (ED; 15 January 2010) and their comparisons with the normal EEJ control day (CD1; 2 January 2010), and the preceding control day (CD2; 14 January 2010). The black lines with stars show the variations in obscuration magnitude. The shaded regions outline the eclipse duration with the two-headed arrows in the middle which signify the centrality of the eclipse at each station.

recovered after the eclipse. However, when we go farther north the smaller VTEC values between the day before the eclipse and the day of the eclipse accentuate. The lowering of plasma at these higher latitude is evidently implying the weakened plasma transport process. The low value of TEC at Shillong and Jaipur during the control days suggests that their latitudes lay beyond the EIA crest in January. This is in agreement with the past studies of Bhuyan and Bhuyan (2009), which illustrates the general behavior of low EEJ strength during the winter solstice. Exceptionally, the VTEC at Jaipur was down in the morning itself prior to the onset of CEJ on the eclipse day. This was quite anomalous. However, a further decrease in VTEC during the eclipse is mainly ascribed to the added recombination associated with the downward plasma motion at Jaipur due to the westward electric field.

### 3.7. Latitudinal variation of TEC

To examine the anomaly strength and its latitudinal extent on the eclipse and control days, hourly averaged VTEC values for the period 09:00–17:00 IST, are plotted against the geomagnetic latitudes of the GPS stations in Fig. 8. It clearly shows that on the day before as well as on the eclipse day, the EIA crest was formed near Bangalore (close to the equator), rather than near higher latitudes around Vizag. This supports the inferences drawn from Fig. 7, i.e., the weakened diffusion of plasma during the eclipse has shifted the crest equatorward. Moreover, the latitudinal variation of TEC should have some contribution from the photo-ionization deviation corresponding to the latitudinal variation of eclipse obscuration though it is small in comparison to the electrodynamic consequences on the eclipse day.

### 3.8. Percentage deviation of TEC

Fig. 9 shows latitudinal plots of percentage deviation of TEC (a) from the preceding day and (b) from the normal EEJ control day, during pre- and post-eclipse as well as during the intermediate phases (initial, main, and recovery) of the eclipse. The reduction started at all the stations right from the initial phase, with the maximum excursion being witnessed during the post-eclipse period. Interestingly, the percentage deviation curves at different phases are more organized if the day before the eclipse is chosen as the control day as opposed to a normal quiet day. This is probably due to the presence of a similar CEJ pattern on the day before of the eclipse day, though the strength of CEJ is relatively stronger on the eclipse day. The other notable feature is that the percentage deviation of the eclipse day VTEC at the equatorial/off-equatorial stations was greater/lesser than the preceding day (CEJ

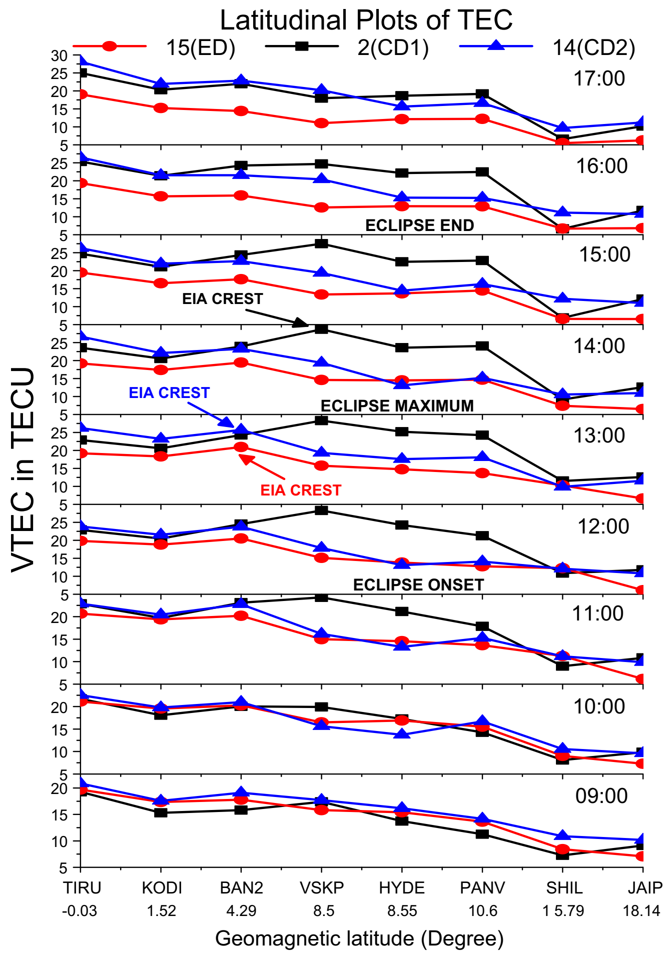


**Fig. 8.** Latitudinal plots of hourly VTEC on the eclipse day (ED; 15 January 2010) and their comparisons with the normal EEJ control day (CD1; 2 January 2010), and the preceding control day (CD2; 14 January 2010). The arrows indicate latitudes of EIA crests on the respective days.

day) in contrast to a normal EEJ day. The pre-eclipse VTEC enhancement is clearly evident on eclipse day if a normal EEJ day is taken as reference. However, the enhancement is less prominent when the reference day is the preceding day. Selecting two different types of control days made for a clear understanding of prevailing equatorial electrodynamics and its effects at the equator and elsewhere, during the eclipse. We presume the maximum negative deviations in VTEC at Vizag were due to a weakened EIA, with the crest moving towards the equator away from its normal latitude near Vizag.

In Table 2, we compare the percentage deviation of VTEC at all the studied stations and the corresponding results at exactly the same or nearby locations carried out by earlier researchers (Galav et al., 2010; Momani and Sulaiman, 2011; Kumar and Singh, 2012; Vyas and Sunda, 2012; Madhav Haridas and Manju, 2012), who selected different quiet/control days as reference days for the same event. The apparent discrepancy between their reports and our results on TEC reduction is due to the difference in control days selection. In light of these divergences from earlier reports, it is evident that the selection of an appropriate control day is crucial, which is particularly true in the equatorial and low latitude region during the solar eclipse.

## 4. Conclusions

The multi-instrument observations from a network of magnetometer, ionosonde and GPS receivers have provided an opportunity to investigate the electrodynamic consequences of the noon-time annular solar eclipse over the equatorial and low latitude region. Further, consideration of the day before (CEJ day) of the eclipse and a regular quiet day (normal EEJ day) as control days allowed a better understanding of the underlying physics.

The study led us to ascertain the faster downward movement of plasma as the primary cause for a simultaneous increase in electron density (foF2) over the equator and a substantially decreased TEC at all other latitudes. Although the substantial decrease in foF1 at eclipse time is clearly related to the eclipse obscuration as expected, the increase in foF2 and lowering of the hmF2 are the major consequences of the eclipse-time downward motion of plasma as confirmed from the magnetometer and ionosonde observations. By comparing with the normal EEJ day it is inferred that the temporary lack of photo-production only played a subdued role as opposed to downward plasma flow due to the westward zonal electric field associated with the CEJ in most part of the day. However, since the downward motion of plasma was also there on the day before of the eclipse, the post-noon foF2 reduction had to be due to the eclipse itself, which interrupted photo-ionization during the hour when it should have been at its peak production time.

In contrast to foF2 level, the eclipse day reveals smaller VTEC at equatorial and farther latitudes than the normal instead of a larger amount on the day before. This seems to be due to the simultaneous lack of plasma production during the eclipse and continued recombination at the lower F-region altitudes. The largest deviations in VTEC from the normal day, at the regular crest latitude are due to the equatorward shifting of the anomaly crest. This is attributable to the poor feeding of the EIA on the day of the eclipse not so much because of the eclipse itself, but rather due to the very strong CEJ. The more organized plots of percentage deviation of TEC during different phases on the eclipse day from the day before as opposed to the deviations from the normal EEJ control day is probably due to the presence of similar CEJ pattern on the eclipse and its day before. The strong CEJ in other words corresponds to the substantial westward zonal electric field, which is the potential driver behind the downward plasma motion and hence the severely weakened fountain effect on the eclipse day. Since a rather strong CEJ was seen also on the days before and after the eclipse as well, it is tempting to attribute the CEJ occurrence and impact on the EIA during the eclipse to the strong gravitational tides generated by the unique Sun-Moon-Earth alignment.

Although the modified ionospheric electrodynamics during the eclipse is predominantly attributed to the weakened/reversed daytime electric field seen through the magnetometer data, the possible origin of the CEJ has not been discussed in earlier studies. Hence, in the present work we suggest the strong gravitational tidal effect does exist on the solar eclipse day, likely to be due to the exceptional alignments of the Sun with the Moon. Moreover, there is also evidence for of exceptional global enhancements in the geomagnetic lunar tides in January due to the equatorial lunar effects (Mayaud, 1977; Stening, 1977). All these situations may modulate the daytime eastward electric field and lead to the CEJ recorded in the magnetometer data. Furthermore, the high pressure in the southern hemisphere during the winter and the low pressure along the eclipse path are also likely to be triggering the CEJ (St.-Maurice et al., 2011). However, the pressure difference due to the eclipse itself is a short-lived phenomena, which plays a subordinate role compared to the accompanying gravitational tides.

The present solar eclipse gave us a unique opportunity to study the large-scale effects of the altered electrodynamics over the equatorial and low latitude Indian region. The consequences of this study should help in better understanding various solar-

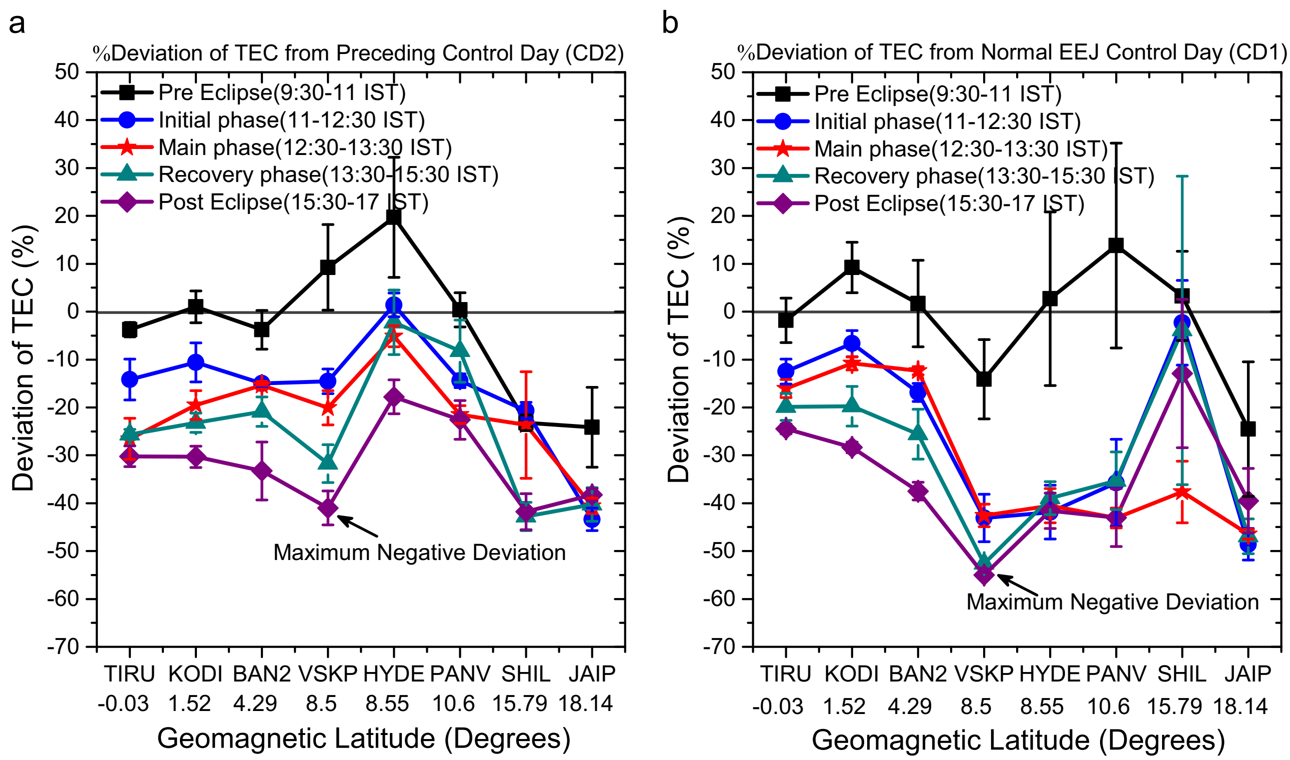


**Fig. 9.** Latitudinal plots of percentage deviation of VTEC on the eclipse day (ED; 15 January 2010) and their comparisons with (a) the preceding control day (CD2; 14 January 2010) and (b) the normal EEJ control day (CD1; 2 January 2010) during the pre-, post- and the intermediate (initial, main and recovery) phases of the eclipse.

terrestrial phenomena and eventually in establishing more realistic regional ionospheric models over the low latitudes.

## Acknowledgments

The authors acknowledge CDDIS for IGS-GPS observation data and broadcast ephemeris files, Director, Indian Institute of Geomagnetism for providing magnetometer data, ionosonde data of Tirunelveli and GPS observation data of permanent GPS stations, and B.C. Bhatt from Indian Institute of Astrophysics for providing Kodaikanal GPS data. The ionosonde data of Trivandrum station is obtained from T.K. Pant, Vikram Sarabhai Space Centre (VSSC), Trivandrum, India. Also, sincere appreciation goes to World Data Center for Geomagnetism, Kyoto for information on geomagnetic indices. The OMNI data (1-min averaged SYM-H, IMF-Bz, and Electric field) were obtained from the GSFC/SPDF OMNIWeb interface at http://omniweb.gsfc.nasa.gov. Three-hourly Kp index is obtained from Space Physics Interactive Data Resource (SPIDR). The authors also thank CODE-University of Bern for GPS satellite inter-frequency biases. The authors also sincerely thank Gopi K. Seemala, Indian Institute of Geomagnetism (previously at Kyoto University Japan) for providing the GPS TEC analysis software used in this study. Our sincere thanks to A. Nishida and Y. Yamazaki for valuable discussions.

## References

Adeniyi, J.O., Radicella, S.M., Adimula, I.A., Willoughby, A.A., Oladipo, O.A., Olawepo, O., 2007. Signature of the 29 March 2006 eclipse on the ionosphere over an equatorial station. J. Geophys. Res. Space Phys. 112 (A6), A06314.
Appleton, E.V., 1946. Two anomalies in the ionosphere. Nature 157, 691.
Bhaskar, A., Purohit, A., Hemalatha, M., Pai, C., Raghav, A., Gurada, C., Radha, S., Yadav, V., Desai, V., Chitnis, A., Sarpotdar, P., Patankar, A., 2011. A study of secondary cosmic ray flux variation during the annular eclipse of 15 January 2010 at Rameswaram, India. Astropart. Phys. 35 (5), 223–229.
Bhaskar, A., Vichare, G., 2013. Characteristics of penetration electric fields to the equatorial ionosphere during southward and northward IMF turnings. J. Geophys. Res. Space Phys. 118 (7), 4696–4709.
Bhuyan, P.K., Bhuyan, K., 2009. The equatorial ionization anomaly at the topside F region of the ionosphere along 75° E. Adv. Space Res. 43 (11), 1676–1682.
Chandra, H., Misra, R., Rastogi, R., 1971. Equatorial ionospheric drift and the electrojet. Planet. Space Sci. 19 (11), 1497–1503.
Chandra, H., Sharma, S., Lele, P.D., Rajaram, G., Hanchinal, A., 2007. Ionospheric measurements during the total solar eclipse of 11 August 1999. Earth Planets Space 59 (1), 59–64.
Chapman, S., 1951. The equatorial electrojet as detected from the abnormal electric current distribution above Huancayo, Peru, and elsewhere. Arch. Meteorol. Geophys. Bioklimatol. Ser. A 4 (1), 368–390.
Choudhary, R.K., St.-Maurice, J.P., Ambili, K.M., Sunda, S., Pathan, B.M., 2011. The impact of the January 15, 2010, annular solar eclipse on the equatorial and low latitude ionospheric densities. J. Geophys. Res. Space Phys. 116 (A9), A09309.
Cohen, E.A., 1984. The study of the effect of solar eclipses on the ionosphere based on satellite beacon observations. Radio Sci. 19 (3), 769–777.
Espenak, F., Anderson, J., 2008. Annular and Total Solar Eclipses of 2010. Technical Report NASA TP-2008-214171, Goddard Space Flight Center, Greenbelt, MD.
Espenak, F., Meeus, J., 2006. Five Year Millennium Canon of Solar Eclipses: −1999 to +3000 (2000 BCE to 3000 CE). NASA Technical Paper. NASA Goddard Space Flight Center.
Evans, J.V., 1965. An F region eclipse. J. Geophys. Res. 70 (1), 131–142.
Galav, P., Sharma, S., Pandey, R., 2010. Total electron content in peninsular India during the eclipse of 15 January 2010. Curr. Sci. 99 (6), 731–732.
Gouin, P., Mayaud, P.N., 1967. A propos de l'existence possible d'un contre electrojet aux latitudes magnetiques equatoriales. Ann. Geophys. 23, 41–47.
Klobuchar, J.A., 1991. Ionospheric Effects on GPS. Early Innovation Columns. GPS World.
Klobuchar, J.A., Whitney, H.E., 1965. Ionospheric electron content measurements during a solar eclipse. J. Geophys. Res. 70 (5), 1254–1257.
Kumar, S., Singh, A.K., 2012. Changes in total electron content (TEC) during the annular solar eclipse of 15 January 2010. Adv. Space Res. 49 (January (1)), 75–82.
Kumar, S., Singh, A.K., Singh, R.P., 2013. Ionospheric response to total solar eclipse of 22 July 2009 in different Indian regions. Ann. Geophys. 31 (9), 1549–1558.
Le, H., Liu, L., Ding, F., Ren, Z., Chen, Y., Wan, W., Ning, B., Xu, G., Wang, M., Li, G., Xiong, B., Hu, L., 2010. Observations and modeling of the ionospheric behaviors over the east Asia zone during the 22 July 2009 solar eclipse. J. Geophys. Res. Space Phys. 115 (A10), A10313.
Lin, C.Y., Liu, J.Y., Lin, C.H., Sun, Y.Y., Araujo-pradere, E.A., Kakinami, Y., 2012. Using the IRI, the MAGIC model, and the co-located ground-based GPS receivers to study ionospheric solar eclipse and storm signatures on July 22, 2009. Earth Planets Space 64 (July (6)), 513–520.

Madhav Haridas, M.K., Manju, G., 2012. On the response of the ionospheric F region over Indian low-latitude station Gadanki to the annular solar eclipse of 15 January 2010. J. Geophys. Res. 117 (A1), A01302.
Manju, G., Madhav Haridas, M.K., Ramkumar, G., Pant, T.K., Sridharan, R., Sreelatha, P., 2014. Gravity wave signatures in the dip equatorial ionosphere-thermosphere system during the annular solar eclipse of 15 January 2010. J. Geophys. Res. Space Phys. 119 (6), 4929–4937.
Manju, G., Sridharan, R., Ravindran, S., Madhav Haridas, M., Pant, T.K., Sreelatha, P., Mohan Kumar, S., 2012. Rocket borne in-situ electron density and neutral wind measurements in the equatorial ionosphere—results from the January 2010 annular solar eclipse campaign from India. J. Atmos. Sol.-Terr. Phys. 86, 56–64.
Manoj, C., Lühr, H., Maus, S., Nagarajan, N., 2006. Evidence for short spatial correlation lengths of the noontime equatorial electrojet inferred from a comparison of satellite and ground magnetic data. J. Geophys. Res. 111 (A11), A11312.
Mayaud, P.N., 1977. The equatorial counter-electrojet—a review of its geomagnetic aspects. J. Atmos. Terr. Phys. 39 (910), 1055–1070.
Momani, M.A., Sulaiman, S., 2011. Ionospheric response to the annular solar eclipse on 15th January 2010 as observed by ionosonde receivers. J. Adv. Sci. Eng. Res. 1 (December), 238–245.
Momani, M.A., Yatim, B., Mohd Ali, M.A., 2010. Ionospheric and geomagnetic response to the total solar eclipse on 1 August 2008 over Northern Hemisphere. J. Geophys. Res. 115 (August (A8)), A08321.
Rastogi, R.G., 1989. The equatorial electrojet: magnetic and ionospheric effects. In: Jacobs, J. (Ed.), Geomagnetism, vol. 3. Academic Press, San Diego, CA, pp. 461–525.
Rastogi, R.G., Klobuchar, J.A., 1990. Ionospheric electron content within the equatorial F2 layer anomaly belt. J. Geophys. Res. Space Phys. 95 (A11), 19045–19052.
Rishbeth, H., Garriott, O.K., 1969. Introduction to Ionospheric Physics. Volume 14 of International Geophysics Series. Academic Press, New York.
Salah, J.E., Oliver, W.L., Foster, J.C., Holt, J.M., Emery, B.a., Roble, R.G., 1986. Observations of the May 30, 1984, annular solar eclipse at Millstone Hill. J. Geophys. Res. 91 (A2), 1651–1660.
Schaer, S., March 1999. Mapping and Predicting the Earth's Ionosphere Using the Global Positioning System (Ph.D. thesis). Astronomical Institute, University of Berne, Berne, Switzerland.
Seemala, G.K., Valladares, C.E., 2011. Statistics of total electron content depletions observed over the South American continent for the year 2008. Radio Sci. 46 (5), RS5019.
Sharma, S., Dashora, N., Galav, P., Pandey, R., 2010. Total solar eclipse of July 22, 2009: its impact on the total electron content and ionospheric electron density in the Indian zone. J. Atmos. Sol.-Terr. Phys. 72 (18), 1387–1392.
Sridharan, R., Devasia, C.V., Jyoti, N., Tiwari, D., Viswanathan, K.S., Subbarao, K.S.V., 2002. Effects of solar eclipse on the electrodynamical processes of the equatorial ionosphere: a case study during 11 August 1999 dusk time total solar eclipse over India. Ann. Geophys. 20 (12), 1977–1985.
Sripathi, S., Bhattacharyya, A., May 2012. Quiet time variability of the GPS TEC and EEJ strength over Indian region associated with major sudden stratospheric warming events during 2005/2006. J. Geophys. Res. 117 (A5), A05305.
St.-Maurice, J.P., Ambili, K.M., Choudhary, R.K., 2011. Local electrodynamics of a solar eclipse at the magnetic equator in the early afternoon hours. Geophys. Res. Lett. 38 (4), L04102.
Stening, R.I., 1977. Ionospheric dynamo calculations with semidiurnal winds. Planet. Space Sci. 25 (11), 1075–1080.
Tomás, A.T., Lühr, H., Rother, M., Manoj, C., Olsen, N., Watari, S., 2008. What are the influences of solar eclipses on the equatorial electrojet? J. Atmos. Sol.-Terr. Phys. 70 (11–12), 1497–1511.
Tsai, H.F., Liu, J.Y., 1999. Ionospheric total electron content response to solar eclipses. J. Geophys. Res. 104 (A6), 12657–12668.
Vyas, B.M., Sunda, S., 2012. The solar eclipse and its associated ionospheric TEC variations over Indian stations on January 15, 2010. Adv. Space Res. 49 (3), 546–555.